

Identifying monopoles on a lattice

Z. Schram* and M. Teper

Theoretical Physics, University of Oxford, 1 Keble Road, Oxford OX1 3NP, United Kingdom

(Received 14 May 1993)

The U(1) Villain model is simulated in three and four dimensions. We locate monopoles using both the conventional DeGrand-Toussaint prescription and the exact prescription as provided by the model itself. The two monopole gases thus obtained are compared, in particular with respect to their confining and percolation properties. In this way we investigate to how strong a coupling the conventional definition of lattice monopoles remains reliable. We show that in the interesting range of “intermediate” couplings ($\beta_v \geq 0.3$) the difference between the two monopole gases can be very well reproduced by a random distribution of dipoles (which possesses trivial long-distance properties). This suggests that the DeGrand-Toussaint prescription can indeed be meaningfully used in studies of, for example, the U(1) phase transition and the monopole mechanism for non-Abelian confinement.

PACS number(s): 11.15.Ha, 14.80.Hv

I. INTRODUCTION

Following the demonstration by Polyakov [1] that monopoles produce linear confinement in three-dimensional U(1) theories, there has been a great deal of interest in studying monopoles and their properties in a variety of lattice field theories. For example, some early studies [2,3] focused on their possible role in driving the deconfining phase transition in U(1) theories in four dimensions. More recently, there has been a great deal of interest [4] in their possible role [5] in non-Abelian confinement and their possible association with a strong-coupling phase for QED [6].

In all the associated numerical work the crucial first step is to locate the monopoles in the fluctuating lattice fields. This is usually done using a prescription first introduced in the pioneering work of DeGrand and Toussaint [3]. As is well known their definition possesses the necessary virtue of becoming exact in the weak-coupling continuum limit. However, for the purposes of the applications listed above this is not enough since they all involve a vacuum which contains strong fluctuations. This raises an obvious question: in such a vacuum do the “monopoles” identified by this prescription have any reality or are they just an artifact of a definition that has become inappropriate once the fields are not smooth almost everywhere? In this paper we attempt to provide a partial answer to this question.

Our approach is to study a model in which there is an unambiguous definition of monopoles at all couplings:

the Villain model. As is well known [1,2,7] the Villain partition function can be written as the product of a Gaussian piece and a monopole gas piece. These monopoles are defined using the extra integer plaquette variables in the model. We perform simulations of the Villain model and for each lattice field configuration we use the conventional DeGrand-Toussaint prescription to identify the monopoles in that configuration. Simultaneously, we identify the “real” monopoles as defined using the plaquette integers. We compare the two resulting gases of monopoles; in particular with respect to those properties that are relevant to the applications listed above. In this way we aim to identify the range of couplings over which the conventional monopole definition retains its intended meaning.

In this paper we shall analyze the Villain model in both three and four Euclidean dimensions. In $D=4$ the monopoles may be viewed as magnetically charged point particles while in $D=3$ they are really instantons. However, since monopoles are the topological singularities of U(1) fields in any three Euclidean dimensions, the monopole field configuration in $D=3$ is identical to that of a static monopole in $D=4$. So, for the sake of simplicity and in an attempt to be consistent with previous work, we shall always speak of “magnetic” monopoles and we shall talk of the $D=3$ fields strengths as being “magnetic” throughout the remainder of this paper; although, of course, in that case two of the three components are really electric. Finally, we remark that the discussion below will be for the $D=3$ case except where explicitly stated otherwise.

II. THE U(1) VILLAIN MODEL

In this section we briefly outline the basic notions of the Villain model and the different ways of defining monopoles within it.

The partition function of the model is [7]

*On leave of absence from Dept. of Theoretical Physics, Kossuth University, H-4010 Debrecen POB. 5, Hungary.

$$Z = \int_{-\pi}^{+\pi} \prod d\theta_\mu(x) \sum_{[l_{\mu\nu}(x)]} \exp \left[-\frac{\beta}{2} \sum_{x,\mu\nu} [\theta_{\mu\nu}(x) - 2\pi l_{\mu\nu}(x)]^2 \right], \quad (1)$$

where

$$\theta_{\mu\nu}(x) = \theta_\mu(x) + \theta_\nu(x + \hat{\mu}) - \theta_\mu(x + \hat{\nu}) - \theta_\nu(x)$$

and β is related to the dimensionless bare coupling g^2 by $\beta = 1/g^2$. In the above expression the θ_μ 's are angle variables $\theta_\mu(x) \in [-\pi, \pi)$, which are defined on the links of the lattice, and the $l_{\mu\nu}$'s are integers, $l_{\mu\nu}(x) \in \mathbb{Z}$, that are defined on the elementary plaquettes of the lattice. As a convenient shorthand we will usually use p rather than μ, ν, x to label plaquettes.

If we regard Eq. (1) as a partition function for the angular variables we see that in the weak-coupling limit it is in the same universality class as the usual plaquette action. Moreover, since it is periodic in the plaquette angle θ_p , Dirac strings will be invisible and the usual arguments motivate the use of the DeGrand-Toussaint prescription to identify monopoles in the weak-coupling limit. This prescription is as follows. The plaquette angle θ_p is decomposed into two parts:

$$\theta_p = \bar{\theta}_p + 2\pi n_p. \quad (2)$$

The first term on the right-hand side of this equation, $\bar{\theta}_p$, lies between $-\pi$ and π and is interpreted as giving the *physical* flux through the plaquette, p . The second term is an integer multiple of 2π , and is taken to represent the net number n_p of Dirac strings passing through the plaquette p . After this decomposition one can use Gauss's law to locate any monopoles: the magnetic charge enclosed by a closed surface is determined either by the total physical flux through this surface or by the sum of the number of Dirac strings, n_p , through it. It is easy to see that using Eq. (2) one gets the same result either way. So in three space-time dimensions, where we have pointlike monopole charges sitting on the sites of the dual lattice, the monopole charge in an elementary cube c is

$$m = \sum_{p \in \partial c} n_p, \quad (3)$$

where the summation is an *oriented* one over the plaquettes that form the boundary of the cube.

The prescription provided by Eqs. (2) and (3) is a general one for any U(1) theory. The Villain model has, however, the unusual property of already possessing a natural definition of monopoles within it. We recall that the partition function can be transformed analytically into a product [1,2,7]

$$Z = Z_{\text{Gauss}} Z_{\text{mon}}, \quad (4)$$

where

$$Z_{\text{Gauss}} \sim \int_{-\infty}^{+\infty} (d\theta_\mu) \exp \left[-\frac{\beta}{2} \sum_p \theta_p^2 \right] \quad (5)$$

and

$$Z_{\text{mon}} \sim \sum_{m \in \mathbb{Z}} \exp \left[-2\pi^2 \beta \sum_{x,y} m(x) v(x-y) m(y) \right], \quad (6)$$

where $v(x-y)$ is a lattice version of a $1/r$ potential.

Clearly, Z_{Gauss} is just a free (lattice) field partition function. Z_{mon} , on the other hand, is the partition function of a gas of "charged" particles interacting via a $1/r$ potential. These "charged" particles are the "monopoles" of the theory. The charge $m(x)$ in Eq. (6) can [7] be simply expressed in terms of the integer variables l_p in Eq. (1):

$$m = \sum_{p \in \partial c} l_p, \quad (7)$$

where again an *oriented* sum is implied.

Suppose we insert a pair of static sources into the theory coupled to the angular variables, θ_μ . If we calculate the potential between these sources as a function of their separation we again find a factorization into Gaussian and monopole pieces. The Gaussian piece provides the usual Coulomb potential while the monopoles lead, at large separations, to a linearly confining potential. This statement is valid for all values of the coupling although it is only in the weak-coupling limit, where the monopoles are dilute and have at most unit charges, and in the strong-coupling limit that analytic calculations [1,7] are feasible.

In four dimensions a similar factorization holds. The monopoles now have world lines and the conservation of magnetic charge means that in a finite periodic volume these world lines will form closed, contractible loops. (If a loop winds around the torus then it can always be paired with another loop such that the *pair* of loops is contractible.) Simple action versus entropy arguments tell us that at weak coupling these loops are small and dilute. Thus in any three-dimensional spatial manifold the monopoles always appear closely paired with corresponding antimonopoles. That is to say, we have a dilute gas of dipoles rather than of monopoles and antimonopoles. A gas of dipoles has no interesting long-distance physics; in particular, it does not confine. If we now increase the coupling the same energy versus entropy arguments suggest that there will be a phase transition in which the monopole loops become unbounded. Our three-dimensional spatial manifold now contains a plasma of monopoles which will produce linear confinement just as it does in three space-time dimensions. This is the phase transition between the strong-coupling confining phase and the weak-coupling deconfined spin-wave phase in the $D=4$ Villain model. It has been argued [2] that similar monopole dynamics drives the corresponding phase transitions in other $D=4$ U(1) theories.

In other models we do not, in general, possess a natural monopole definition analogous to Eq. (7). In such cases once one has identified some U(1) fields one relies on the

DeGrand-Toussaint prescription of Eqs. (2) and (3) to identify monopolelike fluctuations in the lattice $U(1)$ fields. However, the separation in Eq. (2) of θ_p into a physical flux and Dirac strings is only compelling if the fluctuations are so weak that the values of θ_p almost always lie in narrow bands centered around integer multiples of 2π , i.e., if $|\bar{\theta}_p| \ll \pi$. This is what occurs when β is large. In that case it is clear that the Boltzmann factor in Eq. (1) forces n_p in Eq. (2) to be equal to l_p up to exponentially small corrections. And then the monopole definitions in Eqs. (3) and (7) become identical. However, as β is decreased and the field fluctuations become greater, $\bar{\theta}_p$ becomes more evenly distributed and the correlation between the n_p and the l_p weakens. It then becomes unclear to what extent the prescription in Eqs. (2) and (3) is really pin-pointing monopolelike fluctuations.

In the Villain model this question has both a precise meaning and a precise answer. On any given lattice field one can compare the distribution of monopoles obtained using Eqs. (2) and (3) with that obtained using Eq. (7). One can then look at ensemble averages and calculate the properties of the two monopole “gases” obtained using these two different definitions. One can see how significant this difference is for any physical quantity of interest, e.g., the confining string tension. By performing this kind of comparison as a function of β one can see how far into the region of strong coupling one can reliably utilize the DeGrand-Toussaint prescription to identify Villain monopoles. This is what we now turn to.

III. COMPARISON OF THE TWO MONOPOLE DEFINITIONS

We use a Monte-Carlo simulation to create lattice field configurations that are typical of the Villain model for the intermediate range of couplings that most interests us. We use a standard heat-bath algorithm to update the link variables and a Metropolis algorithm to update the plaquette variables. On each of the configurations so obtained we use Eq. (7) to assign an integer $m_V(c)$ to each cube c whose value equals the (Villain) magnetic charge in that cube. (Equivalently, we may imagine assigning this charge to each site on the dual lattice.) In four dimensions we assign an integer-valued monopole current to the links of the dual lattice. We now repeat the procedure with the DeGrand-Toussaint algorithm of Eqs. (2) and (3) and thus obtain a magnetic charge in each cube which we call $m_{DGT}(c)$. Each of the sets $\{m_V(c)\}$ and $\{m_{DGT}(c)\}$ describes a “gas” of monopoles and antimonopoles. Since we are interested in how these two gases differ, it is convenient to introduce a third distribution of monopole charges that is obtained from the difference of the Villain and DeGrand-Toussaint charges:

$$m_{\text{diff}}(c) = m_V(c) - m_{DGT}(c). \quad (8)$$

This “difference” gas contains *all* the available information on how the two monopole definitions differ from each other.

A. Monopole density

In $D=3$ the simplest quantity we can calculate is the fraction of cubes containing a nonzero magnetic charge. In $D=4$ the corresponding quantity is the fraction of dual links carrying a nonzero monopole current. We shall refer to this as the “monopole density” in this paper. (Note that these definitions of the monopole charge and current densities only count multiply charged cubes or links once.)

We recall that this density has two trivial limits. On the one hand, as β increases, the difference between the θ_p and the l_p is increasingly minimized by the Boltzmann weight in Eq. (1), and this means that the n_p will equal the l_p up to corrections that go to zero exponentially with β . On the other hand, for $\beta \rightarrow 0$ the θ_p and l_p cease to be coupled by the Boltzmann factor and the two monopole gases become completely uncorrelated.

We show typical numerical results for the $D=3$ density in Fig. 1 and for the $D=4$ density in Fig. 2. The latter are obtained on 8^4 lattices and the former on lattices ranging in size up to 16^3 . The densities shown display the expected trends as one approaches the weak- and strong-coupling limits. However, what we are really interested in is the intermediate-coupling region relevant to the applications we mentioned earlier. In the $D=4$ case these typically involve the study of monopole properties in the vicinity of the phase transition which occurs near $\beta \approx 0.6$ in the Villain model. This phase transition, shifted and smeared slightly by finite-volume effects, can be clearly seen in the near discontinuity of the Villain density in

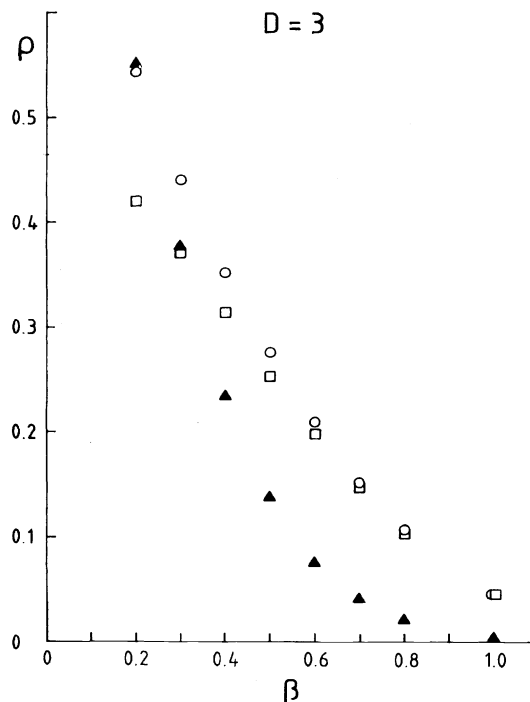


FIG. 1. Fraction, ρ , of cubes with nonzero monopole charge as a function of β in three dimensions; for Villain (\circ), DeGrand-Toussaint (\square), and “difference” (\blacktriangle) monopole gases.

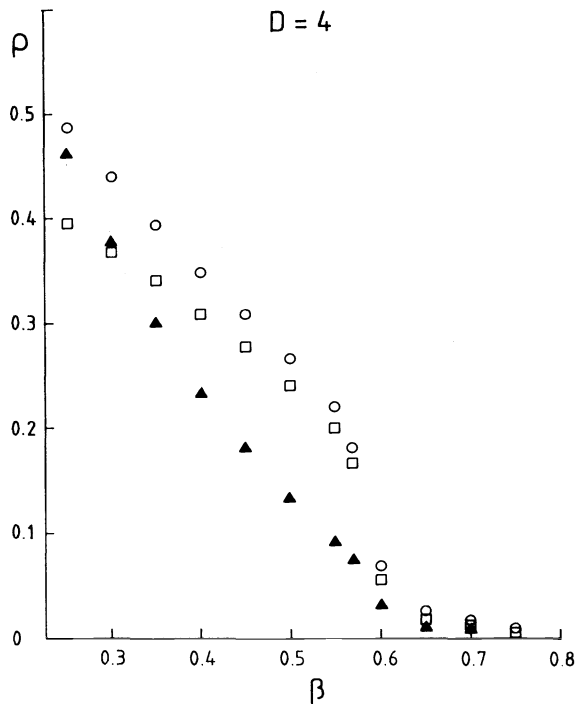


FIG. 2. As in Fig. 1 but for $D=4$.

Fig. 2. We also note that the density of DeGrand-Toussaint monopoles shows an identical behavior with only a small difference in normalization near the phase transition.

So far, so good. However, *average* densities may be a misleading indicator of how different the two gases are. So we also plot the density of the “difference” gas defined in Eq. (8). We see in Fig. 2 that this is, in fact, substantial throughout the interesting range of β . This means that although the *average* number of cubes populated by the two sets of monopoles is rather similar, if we look more closely we find that individual cubes are being assigned very different charges by the two definitions. Is this difference physically important or not? To answer this question we must look more closely at the long-distance properties of the “difference” gas. We shall focus on two such properties; those related to percolation phase transitions and those related to linear confinement.

B. Monopole string tension

If the physics we are interested in relates to confinement then what we need to determine is the contribution of each type of monopole to the string tension σ . Now, σ can be calculated from the area decay of Wilson loops $W(I, J)$, where $I \times J$ is the area of the loop. Because Wilson loops factorize [1,2,7] in the Villain model,

$$W(I, J) = W(I, J)_{\text{Gauss}} W(I, J)_{\text{mon}}, \quad (9)$$

we know that the whole of σ is produced by the Villain monopoles. That this is so has also been verified numeri-

cally [8]. Now to calculate what kind of σ the DeGrand-Toussaint monopole gas would produce, we calculate the expression for $W(I, J)_{\text{mon}}$ in Eq. (9) using the ensemble of monopoles provided by our calculations of $\{m_{\text{DGT}}\}$. And we then do the same for the “difference” gas obtained from $\{m_{\text{diff}}\}$. If the long-distance properties of the conventionally defined monopoles are the same as those of the Villain monopoles then the string tension produced by the m_{diff} gas should be identically zero.

We shall focus here on the $D=3$ case. The calculations of the Wilson loops are straightforward and the technique used is described in the Appendix. We believe that the $D=4$ case should also be straightforward but we have not investigated it, except in a static monopole approximation (see below).

In order to extract string tensions from Wilson loops it is usual to calculate the corresponding Creutz ratios [9], $C(I, J)$:

$$C(I, J) = \frac{W(I, J)W(I-1, J-1)}{W(I, J-1)W(I-1, J)} \sim e^{-\sigma}. \quad (10)$$

These ratios are so defined that perimeter and corner contributions to the Wilson loops cancel out and so one expects that the relevant area term will dominate the value of the Creutz ratio for smaller areas than it would for the Wilson loops themselves.

The Creutz ratios derived from the “difference” and Villain gases are shown in Figs. 3(a) and 3(b), respectively. The latter figure provides reasonable evidence that the Villain gas produces a nonzero string tension. Whether or not Fig. 3(a) provides comparable evidence for the “difference” gas is much less clear: the Creutz ratios show some sign of still increasing for the large areas where the signal disappears into the noise and this leaves open the possibility that the limiting value is unity, corresponding to a zero string tension. Since all these calculations are at relatively strong coupling a much more accurate numerical calculation for the larger areas would be very expensive. So one might imagine relying, instead, on an argument that goes as follows. In the range of β involved the correlation length is already small so one would expect that the asymptotic behavior of the Creutz ratios should set in for small values of the area. (Because a small correlation length implies that the usual perturbative exchanges should be well described by the perimeter and corner terms which cancel in Creutz ratios.) If this is so then we should discount the fact that the Creutz ratios in Fig. 3(a) are showing some sign of still increasing with area when we lose sight of them in the fog of statistical errors. We then conclude that the “difference” gas behaves similarly to the Villain gas, i.e., that it produces a nonzero string tension at all values of β . If we use Eq. (10) to extract a σ_{diff} and a σ_V from the two types of monopole gases, we obtain values of $\sigma_{\text{diff}} \simeq 0.03, 0.08, \text{ and } 0.69$ and $\sigma_V \simeq 0.46, 0.82, \text{ and } 1.61$ at $\beta = 0.7, 0.5, \text{ and } 0.3$, respectively. The apparent fact that $\sigma_{\text{diff}} \neq 0$ would imply, if true, that the conventional DeGrand-Toussaint monopole definition does *not* reliably reproduce the long-distance physics of the underlying Villain mono-

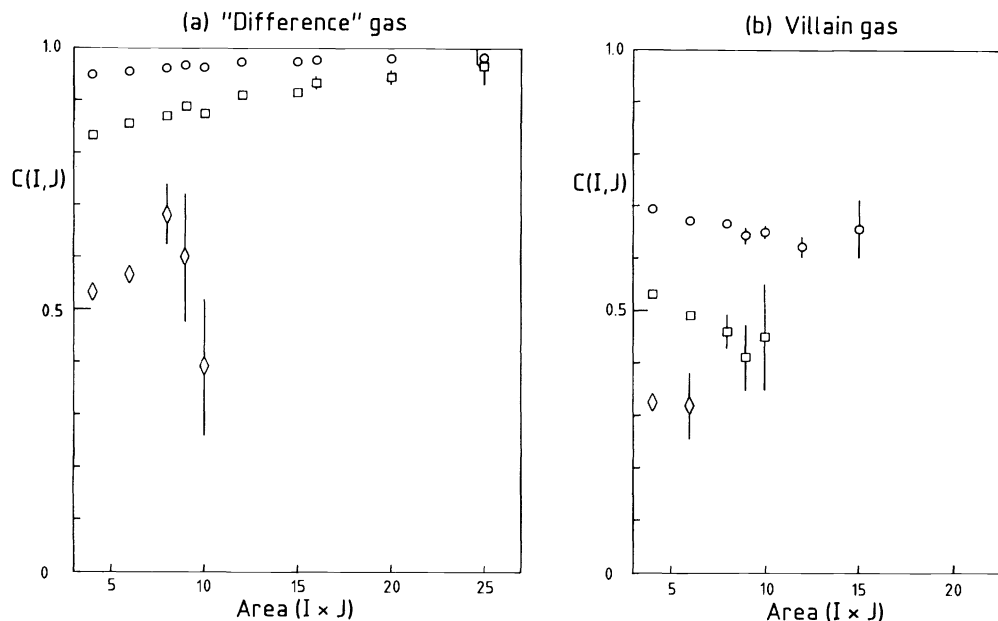


FIG. 3. $D=3$ Creutz ratios at $\beta=0.30$ (\diamond), $\beta=0.50$ (\square), and $\beta=0.70$ (\circ) as produced by (a) the "difference" monopoles and (b) the Villain monopoles.

poles. However, we also note that for $\beta \geq 0.5$ this is a small effect and so one can presumably trust the qualitative physics obtained from the conventionally defined monopoles.

The above discussion suggests that while DeGrand-Toussaint monopoles do not provide a perfect reflection of the confining dynamics of the Villain monopoles, they do do so to a reasonable accuracy in the interesting region around the $D=4$ phase transition and in $D=3$ for values of β outside the strong-coupling limit. This is a modestly reassuring conclusion and, in fact, the one we drew in an earlier publication [10]. However, we now believe that the situation is considerably better than this "minimal" scenario. The reason is as follows. We argued that in our range of β the correlation length is small and so we can extract the string tension from Creutz ratios which involve small areas. This argument is correct for Creutz ratios calculated from the full fluctuating fields but is incorrect if we consider Creutz ratios calculated in a subclass of these fluctuations. A simple example of this is provided by the Creutz ratios calculated using the Villain monopole gas. From the factorization property of Eq. (9) we see that the monopole Creutz ratio is given by the full Creutz ratio divided by the Gaussian Creutz ratio. Now the latter does not have a small correlation length; in fact, it has an *infinite* correlation length. So, in general, the Villain monopole Creutz ratios will converge to the correct string tension only at large values of the area.

As an example, consider Wilson loops of dimension $R \times T$ with $T \gg R$. Then, in $D=3$ at small β ,

$$W_{\text{Gauss}}(R, T) \sim \exp(-cT \ln R).$$

Now the Wilson loop in the full theory satisfies

$$W(R, T) \sim \exp(-\sigma RT)$$

because the dynamical correlation length is small at small β . So Eq. (9) tells us that

$$W_{\text{mon}}(R, T) = \exp(cT \ln R - \sigma RT). \quad (11)$$

This is certainly *not* dominated by the area term for small areas.

For monopole gases other than the Villain one we cannot, of course, perform specific calculations of the above kind. Nonetheless, it is clear that we must jettison the idea that small β means that we only need Creutz ratios for small areas. This presents us with an intractable numerical problem. While we cannot solve this problem we note from Fig. 3 that the trend of the Creutz ratios obtained from the "difference" gas is to *increase* as the area increases and this reassures us that our earlier conclusion [10] constitutes a "worst case scenario" for the DeGrand-Toussaint algorithm.

The above discussion motivates us to explore the possibility that $\sigma_{\text{diff}}=0$. To do so we consider the following simple model in which this is indeed the case. Suppose that the only way that the DeGrand-Toussaint prescription differs from the Villain one is that if a Villain monopole is located in a cube c it will occasionally be misidentified by the DeGrand-Toussaint prescription as being in a cube c' where the latter is randomly chosen from the six neighbors of c . In this case $\{m_{\text{diff}}(c)\}$ will consist of monopoles paired with antimonopoles one lattice spacing apart; i.e., the "difference" gas consists of a gas of randomly oriented dipoles (which can overlap by chance and so produce larger dipoles). Now, one can readily show [11] that such a gas of dipoles produces $\sigma \equiv 0$ for any density of dipoles. Moreover, one can also

show [11] that at large enough β the “difference” gas is precisely of this form. It is therefore not unreasonable to calculate the Creutz ratios that such a difference gas produces and to compare them with the Creutz ratios in Fig. 3(a).

To perform this comparison we proceed as follows. We construct our dipole gas by throwing at random onto the lattice monopoles that are paired with antimonopoles one lattice spacing away. Where two such dipoles overlap parts of them can annihilate and so they can produce, for example, monopoles that are paired with antimonopoles more than one lattice spacing away. So the final number of dipoles on the lattice will be a little different from the initial number placed on it. To compare with Creutz ratios that have been obtained from a monopole gas that has been generated at a given value of β , what we do is to tune the input density of the dipole gas so that the final measured density that this produces equals (within errors) the density of the monopole gas we wish to compare it with. We then calculate Creutz ratios within this dipole gas and compare with those calculated in the appropriate monopole gas. Note that because we use periodic boundary conditions all our monopole gases are globally neutral.

An example of such a comparison, at $\beta=0.50$, is presented in Fig. 4(a). The precision with which the dipole gas reproduces the Creutz ratios obtained from the “difference” gas is quite remarkable. And we obtain similar agreement at $\beta=0.30$ and 0.70 . The significance of this agreement is highlighted if we make a similar comparison with Creutz ratios obtained from the Villain monopole gas at, for example, $\beta=0.70$. There we observe, in Fig. 4(b), complete disagreement. We conclude from this that, although the DeGrand-Toussaint prescription does not faithfully reproduce the distribution of Villain monopoles, the difference is equivalent to a

random gas of dipoles (in the interesting range of couplings)—a *trivial* difference if what one is interested in is linear confinement.

We have also performed some calculations in the $D=4$ theory. The first thing we observe is that in the confining phase the “difference” monopole densities are essentially identical to those of the $D=3$ theory at the *same* value of β . This is so up to the point, close to the phase transition, where our finite-size effects become significant. Above the phase transition the densities are much smaller than in $D=3$ at the same β . To compare the properties of the $D=4$ difference gas to the one in $D=3$ we have calculated the Creutz ratios of Wilson loops in a given time slice precisely as though we were in $D=3$. That is to say, we identify the monopoles in that $D=3$ manifold and calculate the Wilson loops as though we were in three dimensions. (While this would not be the correct thing to do if we wished to calculate the contribution of monopoles to the string tension in four dimensions, we are, nonetheless, probing long-distance properties that are related to confinement.) We find that these Creutz ratios are essentially identical to those of the $D=3$ model at the same value of β as long as we are in the confining phase. (We have, in fact, only investigated $\beta \geq 0.30$.) Thus they can also be accurately reproduced by a gas of dipoles. Above the phase transition the Creutz ratios are unity, within errors. So we conclude that, just as in three dimensions, the difference between Villain and DeGrand-Toussaint monopoles in $D=4$ is *trivial* as far as confinement at intermediate (and small) couplings is concerned.

C. Monopole percolation

A quite different insight into the long-distance behavior of a monopole gas may be obtained from its per-

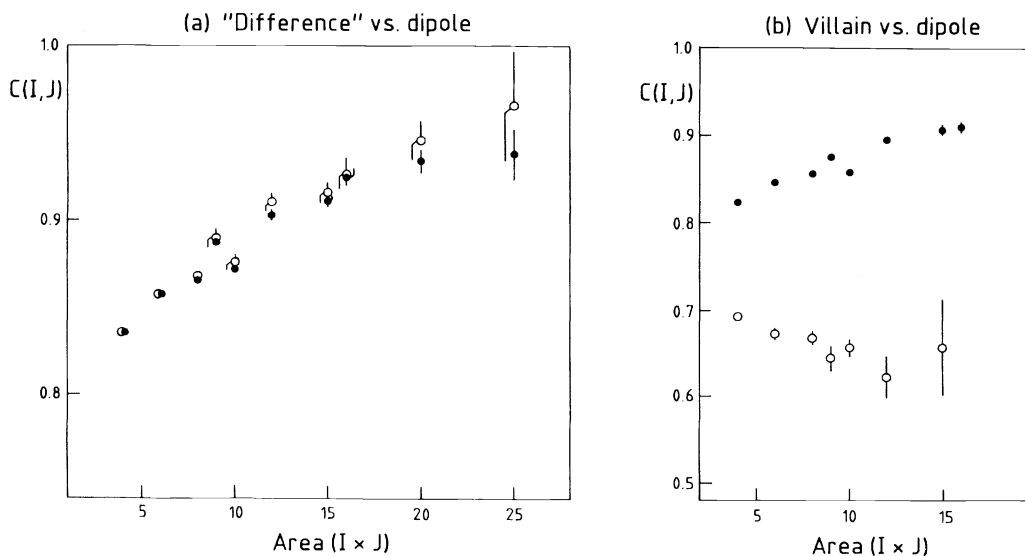


FIG. 4. $D=3$ Creutz ratios as obtained from (a) the “difference” gas at $\beta=0.5$ (\circ) and (b) the Villain gas at $\beta=0.7$ (\circ) are compared with those obtained from dipole gases (\bullet) with the same monopole densities.

colation properties. This is relevant because the bond percolation phenomenon for monopole current networks has been an active area of study recently; in particular, in the context of $D=4$ noncompact lattice QED [12,13]. For us the question this leads to is whether the DeGrand-Toussaint algorithm faithfully reproduces the percolation properties of the Villain monopoles. To answer this question we shall investigate the percolation properties of the various monopole gases in the Villain model. The focus in this section will naturally be on four dimensions.

We first remind the reader of some basic ideas [14]. Two sites on the dual lattice are said to be in the same cluster if there exists between them a continuous path composed of dual links such that all of the links carry a nonzero monopole current. Each monopole current loop is associated with one such nonoverlapping cluster of dual sites. As the density of currents is increased then, in general, at some critical density the largest connected cluster will become infinite in extent and will occupy a finite fraction of the dual lattice. This critical density is called the percolation threshold. The characteristic order parameter for the percolation transition is the expectation value of the quantity

$$\frac{n_{\max}}{n_{\text{tot}}} \equiv \frac{\text{number of sites in the largest cluster}}{\text{total number of connected sites}}. \quad (12)$$

The associated susceptibility is defined as

$$\chi = \left\langle \left[\sum_{i=n_{\min}}^{n_{\max}} g_i i^2 - n_{\max}^2 \right] / n_{\text{tot}} \right\rangle. \quad (13)$$

Here i is the size of a cluster (i.e., the number of dual sites within the cluster), and g_i is the number of clusters of that size that occur on the dual lattice. In the four-dimensional case $n_{\min}=4$ since monopole currents form closed loops and the smallest loop is a plaquette (on a

large enough cubic lattice).

Consider now the $D=4$ Villain model. In Fig. 5 we plot, as a function of β , the values of $\langle n_{\max}/n_{\text{tot}} \rangle$ and χ that we have obtained numerically. We show separately the values obtained using the Villain and DeGrand-Toussaint definitions for the monopole currents. We observe immediately that these possess almost identical percolation properties; at least on a plot of this type. Moreover, the percolation transition occurs at the same value of β as the deconfining phase transition. We also plot the corresponding quantities for the “difference” gas and while we again observe a clear percolation threshold it is equally clear that it occurs nowhere near the phase transition but considerably further into the strong-coupling region.

All these percolation transitions are expected to be second order. It may therefore seem odd that in Fig. 5 some of them appear to be first order. The reason for this is that the deconfining transition is first order and so there is a discontinuity in the monopole current density across it. What apparently happens is that the percolation critical densities lie somewhere in the range spanned by this discontinuity and so the percolation threshold is made to *appear* first order as well. This also tells us that we cannot infer from Fig. 5 that the critical densities for Villain and DeGrand-Toussaint percolation are the same; all we know is that they both lie in the range spanned by the discontinuity.

To resolve the percolation transitions better we take advantage of the fact that in a finite volume, as here, the first-order discontinuity becomes smooth and so we can perform calculations for neighboring values of β that are within the range of the apparent discontinuity in Fig. 5(a). We can then plot $\langle n_{\max}/n_{\text{tot}} \rangle$ and χ not as functions of β but rather as functions of monopole current density. These plots show comparably smooth percolation transitions for all the monopole gases. We show one such plot in Fig. 6. They also show that the critical den-

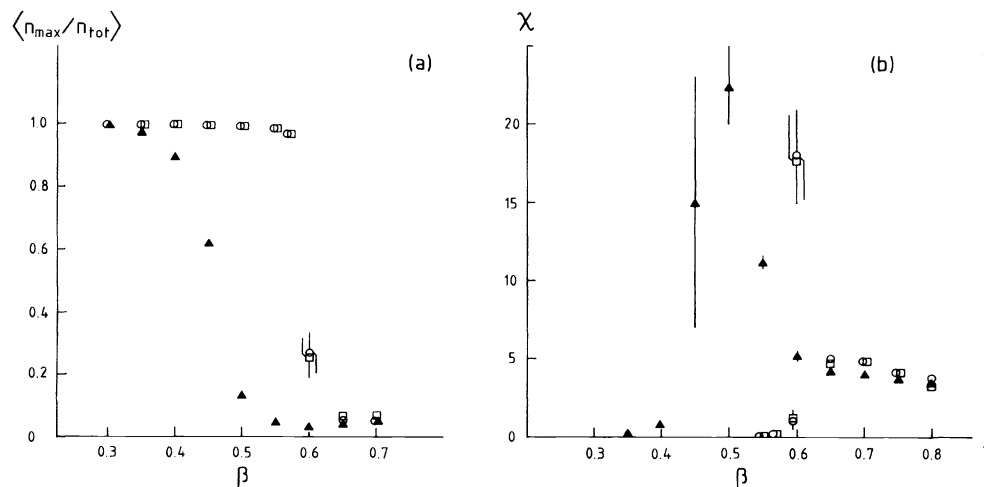


FIG. 5. (a) $\langle n_{\max}/n_{\text{tot}} \rangle$ and (b) the susceptibility for the Villain (\circ), DeGrand-Toussaint (\square), and “difference” (\blacktriangle) monopole gases as a function of β in four dimensions.

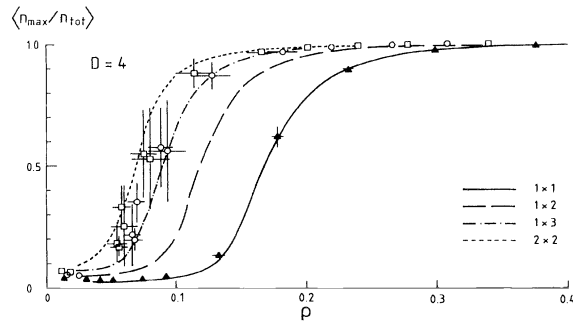


FIG. 6. $\langle n_{\max}/n_{\text{tot}} \rangle$ as a function of the monopole density in $D=4$; for the Villain (\circ), DeGrand-Toussaint (\square) and “difference” (\blacktriangle) monopole gases. The lines interpolate the corresponding values obtained for random gases of monopole loops of various sizes as shown.

sities for the Villain and DeGrand-Toussaint monopoles are indeed very close; although there may be some hint that they are not identical. However, the gap between their critical density and that of the “difference” gas is clearly much greater.

Given that the percolation transition is smooth while the deconfining transition is first order it appears unlikely that the latter is driven by the former in any real sense. This comment does *not* apply to noncompact QED [12,13] where the phase transition is second order.

What do these various percolation transitions tell us about the different monopole gases? We have seen in the previous section that the properties of the $D=3$ “difference” gas are essentially identical to those of a random gas of dipoles. So we try something similar here. The obvious extension of a $D=3$ dipole to $D=4$ is the smallest nontrivial current loop, i.e., on a plaquette. So we create a gas of these “random plaquette currents.” Where they overlap they may, by cancellation, produce loops larger than simple plaquettes. Nonetheless we know that such a gas has no nontrivial long-distance physics. We now calculate $\langle n_{\max}/n_{\text{tot}} \rangle$ and χ within this model, as a function of the average current density. Interpolating the results for $\langle n_{\max}/n_{\text{tot}} \rangle$ gives the continuous solid line in Fig. 6. We see a remarkable coincidence with the values obtained for the “difference” gas. This shows that the percolation properties of the “difference” gas are really those of the most *trivial* possible kind.

It is amusing to generalize the above model of random plaquette currents to current loops that are of a larger size. We have done this separately for 1×2 , 1×3 , and 2×2 monopole loops. In each of these models we have calculated $\langle n_{\max}/n_{\text{tot}} \rangle$ and we have plotted the results as a function of the current density in Fig. 6. We observe that as we increase the loop size the percolation transition approaches that of the Villain monopoles. This provides direct, albeit qualitative, evidence that at the percolation transition of the Villain monopole gas, it is “large” current loops that dominate. Since this percolation threshold coincides with the deconfining transition this tells us that it is large monopole loops that populate

the vacuum as it becomes confining. This is indeed as it should be. Of course, there is a limit to how much we can infer in this vein on our small 8^4 lattices. It would clearly be very interesting to do a finite-size study to see if one could obtain evidence that in large enough volumes there are indeed arbitrarily large loops condensing into the vacuum at the confining phase transition.

Of course, it would be particularly interesting to repeat such calculations for other models where the dynamical role of monopoles is less well understood, for example, across the deconfining phase transition of the $D=4$ U(1) model with a standard plaquette action. But this would take us away from the primary focus of this paper.

Finally, we remark that we have also performed percolation studies of the $D=3$ Villain model. These are less relevant than the $D=4$ case and so we discuss them only briefly. Here we have “site” percolation [14] rather than the “bond” percolation we had in $D=4$. An occupied dual site is one which carries a nonzero magnetic charge and two neighboring sites belong to the same cluster if they are both occupied. The order parameter and the susceptibility can be defined similarly to four dimensions, except that we must set $n_{\min}=2$ in Eq. (13). We have studied site percolation in the three-dimensional Villain model and found that all three monopole gases have percolation transitions, as shown in Fig. 7. Moreover, just as in $D=4$, the transitions appear to occur at the same densities for the Villain and DeGrand-Toussaint monopoles, while the “difference” gas has its transition at a significantly different density. Of course, the Villain model in three dimensions does not possess a phase transition at finite coupling so the presence of these percolation transitions is presumably not related to a change in the long-distance dynamics of the physical system. We have simulated a random dipole gas and, as we see in Fig. 7, this reproduces very precisely the percolation transition of the “difference” gas, implying that here too the differences between the two gases are essentially trivial, at least for the range of intermediate couplings where our calculations are accurate.

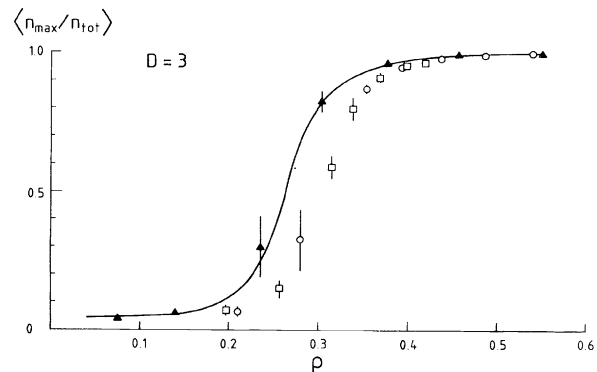


FIG. 7. $\langle n_{\max}/n_{\text{tot}} \rangle$ as a function of the monopole density in $D=3$; for the Villain (\circ), DeGrand-Toussaint (\square), and “difference” (\blacktriangle) monopole gases. The solid line interpolates the corresponding values for a random gas of dipoles.

IV. CONCLUSIONS

In the U(1) Villain model the factorization of the partition function into Gaussian and monopole pieces means that *all* the interesting properties of the model have their origin in the dynamics of the Villain monopoles. Examples are the phase transition in $D=4$ and linear confinement at all β in $D=3$. In this sense the Villain monopoles are the “real” monopoles of the model which the DeGrand-Toussaint prescription should aim to reproduce.

Our calculations have shown that the DeGrand-Toussaint prescription does surprisingly well in this respect. Although there is, superficially, a substantial discrepancy between the monopoles as located by this prescription and the Villain ones, we have seen that, for $\beta \geq 0.3$, this difference can be very accurately reproduced by a random gas of dipoles (in $D=3$) or a random gas of elementary current loops (in $D=4$). In particular, we have shown that this is so for the confining and percolation properties of the “difference” gas.

What can this teach us about the reliability of the DeGrand-Toussaint prescription in other models? It is reasonable to suppose that the extent to which the DeGrand-Toussaint prescription is not performing its desired role is primarily determined by the strength of the vacuum fluctuations. In that case it would be reasonable to expect that the reliability of that prescription in the Villain model should provide some indication of its reliability in other models as long as we perform the comparisons at couplings that lead to comparably strong vacuum fluctuations. The most interesting current applications we are aware of—percolation and confinement around the phase transition in $D=4$ compact and non-compact electromagnetism, confinement in non-Abelian gauge theories—typically involve vacua with fluctuations that correspond to $\beta \geq 0.3$ in the Villain model. Hence this is the range of β upon which we have focused in this paper. Our conclusions should therefore provide reassurance that in these applications the “monopoles” are indeed largely what they are supposed to be.

ACKNOWLEDGMENTS

We have enjoyed useful discussions with Arjan van der Sijs. The numerical calculations were performed, in part, on the RAL Cray under SERC Grant No. GR/H/00772. We acknowledge the Oxford Particle Theory Grant No. SERC GR/F/41501, and one of us (Z.S.) gratefully acknowledges the support of the Royal Society.

APPENDIX: MONOPOLES AND WILSON LOOPS IN THREE DIMENSIONS

We remarked in the text that the partition function of the Villain model can be written as a simple product of spin-wave and monopole pieces, Eqs. (4)–(6), and that the same holds true for Wilson loops, as in Eq. (9). To show [7] this one writes the plaquette integer variable in Eq. (1), $l_{\mu\nu}(x)$, in terms of variables that reside on the links around the plaquette and a scalar field $\phi(z)$ that resides on the dual sites z of the lattice. These link variables are

absorbed with the angular variables to form the spin-wave degrees of freedom. The scalar field may be thought of as the “potential” for the magnetic charge: and indeed the Villain magnetic charge $m(z)$ can be written as

$$m(z) = \sum_{z'=nn(z)} [\phi(z') - \phi(z)], \quad (\text{A1})$$

where the sum is over the nearest neighbors of z , $nn(z)$, of which there are six. (Note that the link variables will automatically sum to zero around the faces of a cube.)

Consider now a Wilson loop W . Take any surface $S(W)$ that spans the Wilson loop. On a cubic lattice this surface is composed of plaquettes $p \in S(W)$. Now let $b(p)$ be the monopole magnetic flux through the plaquette p . If this plaquette is dual to the link labeled by (z, μ) on the dual lattice, then

$$b(p) = 2\pi[\phi(z + \hat{\mu}) - \phi(z)]. \quad (\text{A2})$$

The monopole contribution to the Wilson loop is given by

$$W_{\text{mon}} = \exp \left[i \sum_{p \in S(W)} b(p) \right] \quad (\text{A3})$$

with $b(p)$ as given in Eq. (A2). To obtain the ensemble average $\langle W \rangle_{\text{mon}}$, we average the right-hand side of Eq. (A3) over the ensemble of monopole configurations. For each member of this ensemble the field $\phi(z)$ is obtained as the solution of Eq. (A1). All this can be proved rigorously [7].

So, for a given distribution of magnetic charges we solve Eq. (A1) to obtain the corresponding potential $\phi(z)$ on the dual lattice. We then use Eq. (A2) to calculate the magnetic monopole flux through each plaquette on the lattice. From this we can calculate the flux through any Wilson loop (using the minimal surface for obvious reasons). The value of the Wilson loop is simply the exponential of this flux, as in Eq. (A3). If we now repeat this procedure for each of a Monte Carlo generated ensemble of configurations (where each configuration is specified by a particular distribution of magnetic charges) and average the values thus obtained, then we obtain $\langle W \rangle_{\text{mon}}$ in Eq. (9).

There remains the problem of how to solve Eq. (A1) accurately and efficiently. Our procedure is as follows. For any field ϕ and for any magnetic charge distribution $\{m(z)\}$, we define, for each dual site z ,

$$\delta(z) = \sum_{z'=nn(z)} [\phi(z') - \phi(z)] - m(z). \quad (\text{A4})$$

This quantity is clearly a local measure of how far the ϕ is from being the desired exact solution of Eqs. (A1). We now define the global quantity

$$S = \sum_z \delta^2(z) \geq 0. \quad (\text{A5})$$

The solution of Eq. (A1) can be obtained by minimizing S and we do this by a local iteration starting from the trivial field $\phi(z)=0$. It turns out (as is well known [15]) that in order to minimize a quantity such as S by local iteration it is not efficient to minimize S at each step of the

iteration; rather one should overrelax.

So given a particular distribution of magnetic charges we solve Eq. (A1) for ϕ as follows.

(1) Begin with $\phi(z)=0$ everywhere.

(2) We now pass through the dual lattice one site at a time. Suppose we are at site z . Let us call the current value of $\phi(z)$, $\phi_{\text{old}}(z)$. Define

$$\phi_{\text{new}}(z) = \phi_{\text{old}}(z) + c[\phi_{\text{min}}(z) - \phi_{\text{old}}(z)], \quad (\text{A6})$$

where $\phi_{\text{min}}(z)$ is obtained by minimizing S in Eq. (A5) with $\phi = \phi_{\text{old}}$. Now replace the current value of ϕ at the site z by $\phi_{\text{new}}(z)$. Note that if we set $c=1$ then the new value of $\phi(z)$ is just that which locally minimizes S . But we shall see that this is far from being the most efficient choice.

(3) We repeat the procedure in (2) for all the sites of the dual lattice. This constitutes one iteration. We perform a sequence of such iterations monitoring all the time the values of S and the maximum value of δ^2 anywhere on the lattice. Once these are sufficiently small we stop iterating and the current value of ϕ will be sufficiently close to the desired solution of Eq. (A1).

There remains the choice of the overrelaxation parameter c in Eq. (A6). The ideal procedure would be to determine the best value of c for each monopole configuration at each value of β and for each lattice size; and as a func-

tion of the number of iterations. In our work we found that to obtain a reasonably efficient algorithm it was only necessary to determine c as a function of lattice size. To do so we chose a number of values of c in the range between 1 and 2 and performed 50 iterations at each value to see which led to the smallest final value of S . We used a bisection procedure to home in on the best final value of c . As remarked above we found that this best value worked well for all the monopole configurations on a fixed lattice size. However, it was important to redetermine it when the lattice size was changed.

We have belabored the point about overrelaxation because it makes a real difference. For example, on a 12^3 lattice the value of c we used was $c=1.665$. After 100 iterations this typically led to $S \sim 10^{-6}$ and $\max\{\delta^2(z)\} \leq 10^{-8}$. When we tried the naive value, $c=1$, we found $S \sim 10^{-1}$, a dramatically slower convergence. The value of c we used on our 8^3 lattices was $c=1.585$. This led to $S \sim 10^{-12}$ after 100 iterations. In practice, to benefit from overrelaxation one has to determine the best value of c quite precisely. For example, if we were to use on the 12^3 lattice the value of c that we used on the 8^3 lattice, i.e., $c=1.585$, then we would obtain $S \sim 10^{-3}$ after 100 iterations; which is much worse than what we obtain with the apparently nearby value of $c=1.665$. In our calculations we typically performed 100–200 iterations having checked that this was more than accurate enough to determine the Wilson loops and Creutz ratios.

-
- [1] A. M. Polyakov, Nucl. Phys. **B120**, 429 (1977).
 [2] T. Banks, R. Myerson, and J. Kogut, Nucl. Phys. **B129**, 493 (1977).
 [3] T. DeGrand and D. Toussaint, Phys. Rev. D **22**, 2478 (1980).
 [4] T. Suzuki, in *Lattice '92*, Proceedings of the International Symposium, Amsterdam, The Netherlands, 1992, edited by J. Smit and P. van Baal [Nucl. Phys. B (Proc. Suppl.) **30**, 176 (1993)].
 [5] G. 't Hooft, Nucl. Phys. **B190**, 455 (1981).
 [6] S. Hands, J. Kogut, and A. Kocić, Nucl. Phys. **B357**, 467 (1991).
 [7] A. M. Polyakov, *Gauge Fields and Strings* (Harwood,

- Chur, Switzerland, 1987).
 [8] R. Wensley and J. Stack, Phys. Rev. Lett. **63**, 1764 (1989).
 [9] M. Creutz, *Quarks, Gluons and Lattices* (Cambridge University Press, Cambridge, England, 1983).
 [10] Z. Schram and M. Teper, in *Lattice '92* [4], p. 579.
 [11] T. Copeland, Ph.D. thesis, Oxford, 1990; T. Copeland and M. Teper (unpublished).
 [12] S. Hands and R. Wensley, Phys. Rev. Lett. **63**, 2169 (1989).
 [13] A. Kocić, J. Kogut, and S. Hands, Phys. Lett. B **289**, 400 (1992).
 [14] D. Stauffer, Phys. Rep. **54**, 1 (1979).
 [15] S. Adler, Phys. Rev. D **23**, 2901 (1981).